Nanostructures

Magnetically Separable, Carbon-Supported Nanocatalysts for the Manufacture of Fine Chemicals**

Shik Chi Tsang, Valérie Caps, Ioannis Paraskevas, David Chadwick, and David Thompsett*

In the liquid phase, diffusion and mass-transfer coefficients are orders of magnitude lower than in the gas phase. Consequently, interparticle and intraparticle transport limi-

[*] Prof. Dr. S. C. Tsang, Dr. V. Caps,[+] I. Paraskevas
The Surface and Catalysis Research Centre
School of Chemistry, University of Reading
Whiteknights, Reading, RG6 6AD (UK)
Fax: (+44) 118-931-6632
E-mail: s.c.e.tsang@reading.ac.uk
Prof. Dr. D. Chadwick
Department of Chemical Engineering and Chemical Technology
Imperial College of Sciences, Technology and Medicine
Prince Consort Road, London, SW7 2AZ (UK)
Dr. D. Thompsett
Johnson Matthey Technology Centre
Blounts Court, Sonning Common, Reading, RG4 9NH (UK)
[+] present address:
CNRS
Institut de Recherches sur la Catalyse
2 Avenue Albert Einstein, 69626 Villeurbanne Cedex (France)

[**] This initial work was part of an Institute of Applied Catalysis (iAc (UK)) Foresight Challenge project. We thank the members of iAc steering panels, Professors C. Adams, C. Gent, D. Jackson, P. Davy (Quest Chemicals), and R. Burch (Queen's University of Belfast) for useful discussions and project guidance. S.C.T. would also like to acknowledge further financial support from Johnson Matthey and the EPSRC (GR/N21727). Dr. H. Hobson and Dr. P. Morrall are acknowledged for recording the XRD measurements and XPS spectra, respectively.

Supporting information for this article is available on the WWW under http://www.angewandte.org or from the author.

 DOI: 10.1002/ange.200460552

tations are likely to occur in liquid-phase reactions catalyzed by solid catalysts. Catalytic processes in the liquid phase are important in many areas of the fine and specialty chemicals industries, and the use of solid catalysts means easier catalyst separation and recovery, hence facilitating their reuse. It is widely accepted that a smaller catalyst particle means a higher activity, and a particle with a diameter below 1 μm experiences no significant attrition, (no reduction in particle size).[1] As a result, both the activity and the stability of a solid catalyst suspended in a liquid phase can benefit greatly from the use of small catalyst particles (<1 μm). The main difficulty, however, is that such small particles are almost impossible to separate by conventional means, which can lead to the blocking of filters and valves by the catalyst. The efficient separation of suspended magnetic catalyst bodies from the liquid product by using an external magnetic field offers a solution to this problem and would be of immense interest. There have been some developments on the use of small magnetic bodies to host biological materials and enzymes that can only function under narrow or restricted reaction conditions.[2,3] However, most of these bodies are unstable under the conditions commonly encountered in catalytic fine-chemical synthesis (acidic, basic, corrosive, oxidizing or reducing environments, and elevated temperatures).

Thus, a significant advance in this area would be to produce a catalyst particle that contains a magnetic core totally isolated from the catalytically active part with high magnetization for ease of separation. This advancement may be achieved by completely shielding the inner magnetic core of the particle from the external environment with impermeable coatings; the catalytically active part, located on the external surface of the coating, will then perform its function with no interference from the core. Graphitic shells (carbon cage structures) are ideal "spacers" for the isolation of magnetic particles as the close-packed graphitic networks are both chemically inert and impermeable to most chemicals. These shells could also prevent sintering of metal nanoparticles at high temperatures once they are formed. Enclosing nanomagnets into carbon cages has been attempted previously by arc evaporation,[4] laser irradiation,[5] electron irradiation,[6] the creation of an "opening" followed by filling,[7] or multistep preparation methods by using carbon deposition (from the catalytic decomposition of gaseous carbon sources) onto alumina-supported metal particles followed by selective removal of the alumina.[1,8] These methods, however, suffer from either extremely low yields or low selectivity for the carbon-enclosed magnetic products (other carbon structures) and lead to a very wide size distribution of the particles in a complex matrix; poor control of the size and structure of the magnetic core and carbon coating is also often encountered. A new methodology in catalyst preparation is to adopt a "bottom-up" approach to modify individual catalyst particles.[9]

Herein we report the synthesis of a new class of magnetically separable catalyst carriers, consisting of carbon-encapsulated nanomagnets, based on a simple nanochemistry approach that involves sequential spraying (the complex dissolved in the fine aqueous droplets determines the nature of the solid material obtained), chemical precipitation, and controlled pyrolysis.[10] We found that well-defined, nanometer-sized magnetic alloy particles, enclosed in quasi-spherical graphitic shells, were obtained in large quantities without the use of any solid supporting material. The carbon-protected nanomagnets used as carriers for catalytically active species (Pd nanoparticles) have a higher activity than commercial carbon-supported catalysts. The total encapsulation of the magnetic core in a carbon network also allows direct handling of intrinsically sensitive magnetic materials (FeNi, Fe_3C) in acidic solution and in air (by protecting them from decomposition), hence separation of these nanocatalysts in an external magnetic field can be achieved.

In a typical synthesis, spraying an aqueous solution of sodium nitroferricyanide (obtained by injecting nickel nitrate solution into the head space of ammonia vapor, followed by pyrolysis of the resultant precipitate at elevated temperatures) leads to iron–nickel alloy nanoparticles with a narrow size distribution. The X-ray diffraction (XRD) pattern (Figure 1), with reflections at $2\theta = 43°$, 51°, and 75°, clearly

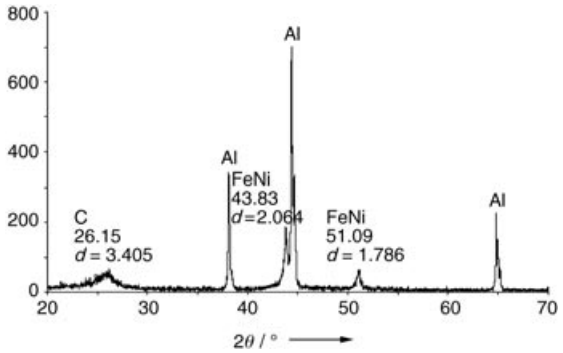

Figure 1. XRD pattern of a carbon-coated, nanometer-sized FeNi magnetic alloy.

indicates the presence of a crystalline mixed Fe–Ni alloy phase. However, it is difficult to assign a precise phase from the XRD pattern—the peaks are very broad—since the 2θ values are very similar to the crystallographic parameters of cubic iron nickel (FeNi; International Centre for Powder Diffraction Source (JCPDS 1996) no. 47-1417, $a = 3.5406$ Å), cubic $FeNi_3$ (JCPDS no. 38-0419, $a = 3.545$ Å), and cubic $Fe_{0.64}Ni_{0.36}$ (JCPDS no. 47-1405, $a = 3.5922$ Å). An average crystallite size of 11 ± 3 nm was calculated from the Scherrer equation. The small, broad hump at $2\theta = 26°$ is attributed to small quantities of graphitic structures a few atomic layers thick, thus leading to a severe peak broadening. It is interesting to note that subsequent treatment of the sample with concentrated hydrochloric acid (boiling for 4 h), which should dissolve unprotected alloy particles, leaves the diffraction pattern unchanged. This result clearly suggests that the alloy particles are protected by some kind of acid-resistant coating. Figure 2a shows a typical TEM micrograph of the spray-precipitation sample (before pyrolysis); nanoscopic particles embedded in an amorphous matrix can clearly be observed. These particles, which are uniform in size, contain both Fe and Ni (~1:1 atomic ratio suggesting a predominant

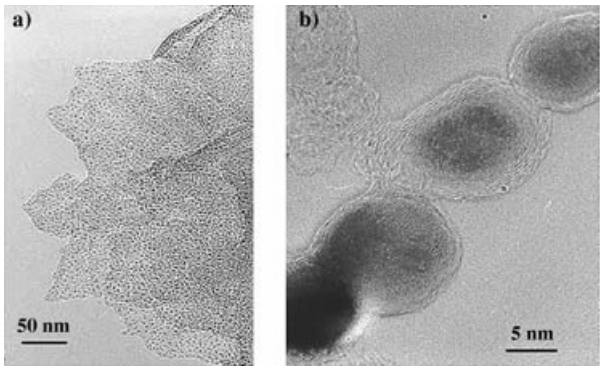

Figure 2. TEM micrograph of carbon-encapsulated FeNi particles deposited on carbon film (×152000 magnification; left) and a high-resolution TEM micrograph of three typical particles (×3100000; right).

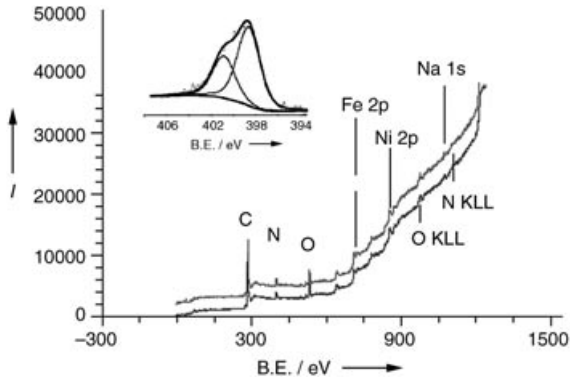

Figure 3. XPS spectrum (and N 1s region; inset) of carbon-coated FeNi nanoparticles.

FeNi phase) as confirmed by energy-dispersive X-ray (EDX) spectroscopy. A majority of the particles are indeed in the size range 10–15 nm. A high-resolution TEM micrograph (Figure 2b) taken after pyrolysis indicates that all the particles are encapsulated by thin, quasi-spherical carbon structures. A detailed examination of these carbon coatings shows that, in many cases, lattice fringes similar to those of graphite (about 3.4 Å) can be traced all around the particles, suggesting concentric carbon-shelled structures. This is in good agreement with the presence of the small, broad graphite peak in the XRD pattern. Prolonged exposure of the selected area to an electron beam (< 60 s) ruled out the possibility that carbon-shell formation occurs upon electron-beam illumination.[6] Thermogravimetric experiments indicate that a typical carbon-protected FeNi sample displays an extremely high alloy content (67.01 wt.%) after acid treatment. These graphite-encapsulated particles can also be found embedded in an external, amorphous carbon coating (the relative size of alloy core and external carbon coating are found to depend on the amount of metal precursors and poly(vinyl alcohol) (PVAL) used). Thus, a good degree of tailoring of the metal core and carbon coating is clearly possible (see also the Supporting Information). It is thought that during the heat treatment in inert gas the cyanide groups play a major role in the reduction of the mixed Fe/Ni-containing seeds, thus allowing both alloy formation and alloy encapsulation, while the added poly(vinyl alcohol), which is known to decompose readily at low temperatures (> 393 K), would provide the amorphous carbon in which the particles are embedded.

Figure 3 shows X-ray photoelecton spectroscopy (XPS) survey spectra of the pyrolyzed sample before and after an in situ heat treatment at 523 K (upper line) for 30 minutes (desorption of contaminants). No major changes are detected and no charging effect is observed on the sample. The peaks are directly referenced to the amorphous carbon (C 1s) peak at 284.6 eV.

It appears that the surface (or the first few atomic layers) consists of pure carbon containing a small number of heteroatoms (O, N, Na, Fe, and Ni)—we detected small signals of Fe and Ni 2p and Auger peaks, with the C/Fe and C/Ni atomic ratios being around 0.05. This fact agrees with the TEM images, which show that the Fe/Ni nanoparticles are totally encapsulated by carbon cages after heat treatment at 1173 K under nitrogen. The binding energies of these exposed Fe and Ni species suggest that they are unlikely to be in the metallic state. An oxygen signal is also found, although it is not yet clear whether this oxygen atom is bound to the exposed iron/nickel species (as surface metal-oxide contaminants before the acid treatment), or to nitrogen or carbon atoms. There are also traces of sodium (Na 1s peak) in the pyrolyzed sample, which probably come from the iron precursor used. It is interesting to note that a nitrogen signal is also observed. The surface contains nitrogen atoms in an ratio to carbon atoms of 43:3. The N 1s region (Figure 3 insert) contains a main peak at 398.6 eV with a shoulder at 400.8 eV. It has been reported previously that an N 1s signal at 401 eV is characteristic of nitrogen atoms present in graphene sheets.[11] We therefore concluded that a small number of nitrogen atoms are incorporated into the graphene network. It has also been reported that a strong peak at 398 eV with a shoulder at 400 eV is due to different C–N bonding (C=N and C–N). Hence we believe that the carbon coating formed around the alloy particles during the heat treatment at 1173 K has a graphite-like structure containing some nitrogen atoms. Nitrogen incorporation (from cyanide pyrolysis) into graphene layers is known to cause curvature of the graphitic planes, which in this case results in encapsulation.[12] Thus, 7% of the surface atoms of our carbon coatings is made up of nitrogen atoms, which makes these encapsulated particles fundamentally and structurally different from those formed by traditional carbon-deposition methods, whose carbon shells contains only carbon atoms and hence are made up of essentially planar graphite plates.

A variety of iron-based binary alloys (FeCu, FeCo, FeNi) were synthesized in this manner. It is interesting to note that when calcium nitrate (Fe/Ca) was used, a very high concentration of carbon-encapsulated nanoparticles with a very narrow size distribution was found. The XRD spectrum (see the Supporting Information) shows that this sample consists of Fe_3C nanoparticles encapsulated in concentric graphitic carbon layers with a small amount of $CaCN_2$ as background matrix. TEM micrographs of the sample after pyrolysis show that the iron-carbide nanoparticles are encapsulated in graphitic carbon (see Supporting Information), with the amorphous calcium-containing phase forming matrices

between the graphite-coated, iron-carbide particles. We attribute this to the fact that calcium does not form a stable alloy with iron (compared to FeNi) but its presence along with the Fe-based nanoparticles protects the composite material from sintering during the heat treatment under nitrogen, hence providing a very high concentration of carbon-coated, iron-containing nanoparticles with a homogeneous size. Microanalysis of the product shows that it contains Ca (35.49 wt.%) and Fe (29.57 wt.%); the rest is carbon. After the acid treatment, selective removal of the calcium-containing matrix releases the tiny, colloidal, graphitic-carbon-encapsulated, magnetic Fe_3C nanoparticles (as confirmed by XRD). These carbon-coated carbide particles contain almost 10.89 wt.% Fe and have a low Ca content (< 1%). All known iron-carbide phases—Fe_2C, $Fe_{2.2}C$, Fe_5C_2, and Fe_3C—are ferromagnetic and display a high magnetization. Fe_3C, in particular, is known to give a high magnetic response but its extreme acid and air sensitivity limits its uses. It is therefore of great interest that this simple technique can be used to prepare large quantities of air- and acid-stable carbon-encapsulated iron carbide.

Figure 4 shows the experimentally measured saturation magnetization of some typical samples. In the case of Fe/Ca, Fe_3C is the predominant phase. It can be seen that the carbon-protected magnetic alloy particles all display negligible magnetic hysteresis (a high magnetization response but with no magnetic aggregation of the fine particles in solution in the absence of a nonhomogeneous magnetic field), hence they are well suited as magnetic catalyst-support particles.

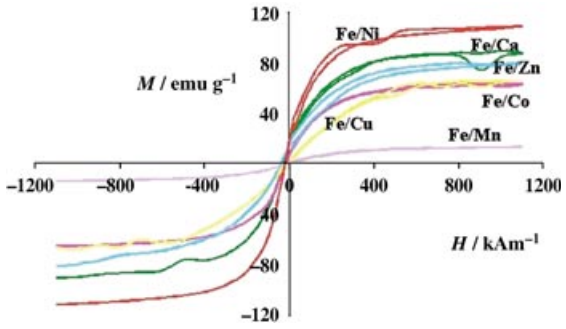

Figure 4. The carbon-protected, Fe-based magnetic particles (metal, alloy, carbide, or their mixtures) all display negligible magnetic hysteresis (high magnetization response with no magneto aggregation of the fine particles in solution in the absence of a nonhomogeneous magnetic field).

Typically, the magnetization of the carbon-coated FeNi nanoparticles reaches saturation when fields above 1000 Oe are applied. A saturation magnetization of 110 emu per gram of the sample is attained; thus, taking into account the alloy (67.01 wt.%), which is the main contributor to the magnetization—the contribution of the graphite jacket is thought to be insignificant relative to the central soft magnetic Fe–Ni core—the saturation magnetization of this material per gram of alloy would be 165 emu g^{-1}. Values of 156 emu g^{-1}[1] have been reported in the literature for the saturation magnetization of bulk nickel–iron alloys with a Ni/Fe ratio of 1. Hence, within experimental error, this encapsulated alloy material appears to display a similar saturation magnetization to the bulk stoichiometric alloy.

The preliminary results shown in Table 1 reveal that the magnetic nanocatalyst is twice as active for hydrogenation of nitrobenzene than a commercial catalyst (Johnson–Matthey)

Table 1: Initial rates of nitrobenzene hydrogenation for two Pd samples.

Catalyst	Initial rate[a]	Mass of catalyst [mg]
5% Pd/C (with Fe-Ni magnetic core)	1.529	32
5% Pd/C (Johnson Matthey powder catalyst)	0.835	50

[a] μmol of nitrobenzene converted into aniline per second.

with the same metal loading, and with a lower amount of catalyst used. We attribute this higher activity of Pd deposited on carbon-coated nanomagnets to the absence of intraparticle mass-transfer limitations and to the better Pd dispersion on the nanometer-sized carbon particles (colloidally dispersed in the solvent) than on the micrometer-sized commercial catalyst powder. The flocculation of the nanometer-sized magnetic catalyst particles from solution is easily achieved within a few minutes by applying an external magnetic field (H_{max} = 38 MG Oe), which facilitates its separation from the product solution.

In summary, we have shown that carbon-encapsulated, iron-based magnetic nanometer-sized particles (10–30 nm, tunable depending on the amount of precursors used) in quasi-spherical carbon shells can be prepared in large quantities by a simple synthetic technique. A unique advantage of the external graphitic carbon surface is that it isolates and protects the magnetic core from destructive reactions with the environment, thus a wide range of experimental conditions can now be used for catalytic synthesis of fine chemicals. The carbon surface can be functionalized with different types of standard catalysts (metal clusters, homogeneous catalysts, enzymes). Hence, these nanocomposite catalysts are an important new development in using solid catalysts for the production of fine chemicals in liquid-phase reactions. Apart from catalytic applications, other useful applications of such carbon-protected, nanometer-sized particles may also be expected in several areas of the nanotechnology field.

Experimental Section

Sodium nitroferricyanide(III) dihydrate [$Na_2Fe(CN)_5NO{\cdot}2H_2O$] (2 g), one molar equivalent of metal nitrate [$M(NO_3)_2{\cdot}xH_2O$; M = Ni, Ca, Mn, Zn, Cu], and poly(vinyl alcohol) (PVAL) as a carbon source (optional, MW 31000–50000) were mixed together in of deionized water (100 mL) at room temperature. This solution was passed through a pneumatic sprayer head kept at a pressure of 1.38×10^5 Pa of nitrogen gas. The fine mist produced (submicrometer-sized droplets) was sprayed into the headspace of a jar filled with saturated ammonia solution (0.88 sg). The fine droplets immediately formed a solid precipitate upon coming into contact with the ammonia (vapor and solution). This solid was collected, washed thoroughly with

deionoized water, dried, and heated to 1173 K under a nitrogen atmosphere for 10 h. The surface of the carbon-encapsulated alloy particles prepared was functionalized with -OH or -COOH groups (confirmed by infrared spectroscopy) by immersing them in boiling concentrated HCl (acid treatment) or a dilute bleach ($NaOCl + H_2O_2$) solution for 4 h and then isolated, washed, and dried.

XPS spectra were recorded on a VSW photoelectron spectrometer with Mg $K\alpha$ radiation (1253.6 eV) equipped with a 100 mm concentric hemispherical analyzer, operating at a constant pass energy in ultrahigh vacuum (1.33×10^{-7} Pa). A survey scan (covering the whole energy range from 1400 to 0 eV) was recorded to determine the position of the peaks. A detailed XPS survey was then recorded as well as detailed scans of the C 1s, O 1s and N 1s regions. No charge effect was observed and the binding energies were directly referenced to the carbon C 1s peak at 284.6 eV. All binding energies are given with an uncertainty of 0.2 eV.

Magnetic measurements were performed by using a vibrating sample magnetometer (VSM), which consists of an electromagnet (maximum applied field of $\pm 1200\ kA\,m^{-1}$) with a sample cell holder vibrating between two pole faces. The VSM measures the difference in magnetic induction between a region of free space with and without the sample as it vibrates thus giving a direct measure of the magnetization M. While the sample is in the magnetic field the magnetic induction is $B_M = \mu_0(H + M)$ and as the sample is moved away this changes to $B_0 = \mu_0 H$, which gives the change in magnetic induction as $\Delta B = \mu_0 M$, in which B is the magnetic induction, H is the magnetic field, M is the magnetization, and μ_0 is the permeability of free space.

To illustrate the use of these carbon-encapsulated nanoalloys as catalyst support, 5 wt. % palladium was deposited onto them by a wet impregnation of $[Pd(acac)_2]$ in acetone. Their catalytic activity was studied for the hydrogenation of nitrobenzene. Nitrobenzene (6.5 mL, 63 mmol) was dissolved in isopropanol (IPA; 125 mL) and placed in a glass beaker inside a 300 mL Parr reactor. The carbon-based catalyst (30 mg) was then added. The reactor was purged with a nitrogen flow for 5 min followed by intermittent purges with pure H_2 at 2×10^6 Pa. The reactor was kept at a pressure of 2×10^6 Pa H_2 and heated up to 353 K with constant stirring (560 rpm). Under these conditions, external mass limitations (such as H_2 solubility and diffusion of substrates from solution to catalytically active sites on solid surfaces) were not anticipated. Samples (< 1 mL) were collected at different times from the reactor by using the internal sampling dip tube without disturbing the ongoing reaction. The samples were analyzed; aniline was the only product observed.

Received: May 4, 2004

Keywords: carbon coating · cyanides · heterogeneous catalysis · magnetic properties · nanomagnets

[1] W. Teunissen, A. A. Bol, J. W. Geus, *Catal. Today* **1999**, *48*, 329.
[2] M. T. Reetz, A. Zonta, V. Vijayakrishnan, K. Schimossek, *J. Mol. Catal. A* **1998**, *134*, 251.
[3] X. Gao, K. M. K. Yu, K. Tam, S. C. Tsang, *Chem. Commun.* **2003**, 2998.
[4] V. P. Dravid, J. J. Host, M. H. Teng, B. E. J. Hwang, D. L. Johnson, T. O. Mason, J. R. Weertman, *Nature* **1995**, *374*, 602.
[5] J. R. Heath, S. C. O'Brien, Q. Zhang, Y. Liu, R. F. Curl, H. W. Kroto, F. K. Tittel, R. E. Smalley, *J. Am. Chem. Soc.* **1985**, *107*, 359.
[6] D. Ugarte, *Chem. Phys. Lett.* **1993**, *209*, 99.
[7] S. C. Tsang, Y. K. Chen, P. J. F. Harris, M. L. H. Green, *Nature* **1994**, *372*, 159.
[8] W. Teunissen, Ph.D. Thesis, Universiteit Utrecht (The Netherlands), **2000**.
[9] K. M. K. Yu, C. M. Y. Yeung, D. Thompsett, S. C. Tsang, *J. Phys. Chem. B* **2003**, *107*, 5737.
[10] "Microparticles and methods of making them": V. Caps, S. C. Tsang (The Institute of Applied Catalysis, UK), PCT Int. Appl. WO 2003057626A1, **2003**.
[11] V. N. Khabashesku, J. L. Margrave, K. Waters, J. A. Schultz, *Thin Solid Films* **2000**, *381*, 62.
[12] S. C. Tsang, J. Qiu, P. J. F. Harris, Q. J. Fu, N. Zhang, *Chem. Phys. Lett.* **2000**, *322*, 553.

